Intrinsic vs Laboratory Frame Description of the Deformed Nucleus ^{48}Cr

E. Caurier,[1] J. L. Egido,[2] G. Martínez-Pinedo,[2] A. Poves,[2] J. Retamosa,[2] L. M. Robledo,[2] and A. P. Zuker[1,2]

[1]*Physique Théorique, Centre de Recherches Nucleaires, Bât 40/1, BP28 F-67037, Strasbourg Cedex-2, France*
[2]*Departamento de Física Teórica C-XI, Universidad Autónoma de Madrid, E–28049 Madrid, Spain*

(Received 16 June 1995)

The collective yrast band of the nucleus ^{48}Cr is studied using the spherical shell model and the Hartree-Fock-Bogoliubov (HFB) method. Both approaches produce basically the same axially symmetric intrinsic state up to the—accurately reproduced—observed backbending. Agreement between both calculations extends to most observables. The only significant discrepancy comes from the static moments of inertia and can be attributed to the need of a more refined treatment of pairing correlations in the HFB calculation.

The study of the collective behavior of deformed nuclei is a classical problem in nuclear physics. Traditionally, mean field descriptions in the intrinsic frame have been favored, as they take advantage naturally of the spontaneous breakdown of rotational symmetry. The price to pay for the gain in physical insight is the loss of angular momentum as a good quantum number.

In the laboratory frame description, as provided by spherical shell model calculations (SM), angular momentum is conserved but the physical insight, associated with the existence of an intrinsic state, is lost, except in the very rare cases where Elliott's SU(3) symmetry [1] operates. Furthermore, the approach suffers from numerical limitations. Hence, so far, it has been implemented mostly in regions such as the p and sd shells where the number of active particles is too small for collective features to become dominant. Nonetheless, there are a few nuclei—such as ^{20}Ne and ^{24}Mg—that are well reproduced by the SM calculations and do exhibit collective properties, whose origin can be traced to the approximate validity of the SU(3) symmetry, for which the relationship between the intrinsic and laboratory frame descriptions is well understood.

In regions where the SU(3) symmetry is poorly respected, as in the pf shell [2], the study of potentially good "rotors" was impaired by lack of experimental evidence, and by the difficulty of an exact SM treatment beyond five active particles. The situation has changed through recent measurements [3] demonstrating that ^{48}Cr is a good rotor up to spin $J = 10$ where the yrast band bends back. This behavior is reminiscent of the situation in much heavier deformed nuclei. Simultaneously, full pf calculations [4] have become available, which reproduce in detail the observed properties of $A = 48$ isobars, and, in particular, those of ^{48}Cr.

Therefore, this nucleus provides a unique testing ground to compare the SM (laboratory frame) description of permanent deformation with cranked Hartree-Fock-Bogoliubov (CHFB) calculations [5] with the finite range density dependent Gogny force [6], which represent one of the best (self-consistent) formulations of the intrinsic frame approach.

From the comparison it should be possible to obtain a better understanding of the intrinsic structure of the SM solutions, which in turn may indicate in what sense the CHFB description falls short of an exact one.

Computational procedures.—In the spherical shell model (SM) ^{48}Cr is described in a $0\hbar\omega$ space, i.e., eight particles are allowed to occupy all the states available in the pf shell (1963 461 states). The effective interaction is given by a minimally modified version of the Kuo-Brown G matrix [7] denoted KB3 in [4]. The single particle energies are taken from the ^{41}Ca experimental spectrum. The effect of core polarization on the quadrupole properties is taken into account by the use of effective charges $q_\pi = 1.5$, $q_\nu = 0.5$. The Hamiltonian is treated by the Lanczos method and diagonalized by the code ANTOINE [8].

In the intrinsic frame calculations we have used the self-consistent CHFB method with the density dependent Gogny force. The CHFB equations determining the mean field intrinsic state $|\phi_\omega\rangle$ are obtained by imposing the condition that the mean value of the Routhian be stationary against small variations of the intrinsic state, i.e.,

$$\delta\langle\phi_\omega|\hat{H} - \omega\hat{J}_x - \lambda_N\hat{N} - \lambda_Z\hat{Z}|\phi_\omega\rangle = 0. \quad (1)$$

The Lagrange multipliers ω, λ_N, and λ_Z are determined by the usual angular momentum and particle number constraints $\langle\phi_\omega|\hat{J}_x|\phi_\omega\rangle = \sqrt{I(I+1)}$, $\langle\phi_\omega|\hat{N}|\phi_\omega\rangle = N$, and $\langle\phi_\omega|\hat{Z}|\phi_\omega\rangle = Z$.

The HFB wave functions have been expanded in a triaxial harmonic oscillator basis $|n_x n_y n_z\rangle$ with different oscillator lengths. Ten oscillator shells are included in order to ensure the convergence of the mean field results. The parameters of the Gogny force used in this calculation were adjusted more than 10 years ago to reproduce ground state bulk properties of nuclei (DS1 set [9]). Without further changes, this force has proven capable of describing successfully many phenomena, and, in particular, high spin behavior [5].

In order to understand more qualitatively the physics involved and to make contact with the shell model calculations we have computed the following quantities in a spherical representation of the basis: The "fractional shell occupancy"

$$\nu(n, l, j) = \frac{1}{2j + 1} \sum_{m=-j}^{m=j} \langle \phi_\omega | c_{nljm}^\dagger c_{nljm} | \phi_\omega \rangle, \quad (2)$$

the "shell contribution to $\langle J_x \rangle$"

$$j_x(n, l, j) = \sum_{m,m'} (J_x)_{(nljm),(nljm')} \langle \phi_\omega | c_{nljm}^\dagger c_{nljm'} | \phi_\omega \rangle, \quad (3)$$

and the "shell contribution to the quadrupole moment"

$$Q_{20}(n, l, j; n', l', j')$$
$$= \sum_{m,m'} (q_{20})_{(nljm),(n'l'j'm')} \langle \phi_\omega | c_{nljm}^\dagger c_{n'l'j'm'} | \phi_\omega \rangle. \quad (4)$$

In the above formulas $| \phi_\omega \rangle$ is the intrinsic CHFB wave function expressed in the triaxial basis and $c_{nljm}^\dagger$ are the operators creating a particle in the harmonic oscillator orbit $| nljm \rangle$ with oscillator length $b_0 = (b_x b_y b_z)^{1/3}$. In order to obtain these quantities the triaxial basis has been expanded in a spherical one following a procedure similar to that of Ref. [10]. As the triaxial basis has, in general, different oscillator lengths the expansion contains in principle an infinite number of terms. In our case, an efficient truncation is obtained by allowing the spherical basis to contain four major shells beyond those in the triaxial basis. The convergence of the truncation has been checked by comparing $\sum_{nlj} (2j + 1)\nu(nlj)$, $\sum_{nlj} j_x(nlj)$, and $\sum_{nlj;n'l'j'} q_{20}(nlj; n'l'j')$ with $\langle N \rangle$, $\langle J_x \rangle$, and $\langle Q_{20} \rangle$, respectively. The differences are typically of the order of 0.01%.

Energetics.—In Fig. 1 the SM, CHFB, and experimental gamma ray energies $E_\gamma(J) = E(J) - E(J - 2)$ are plotted as a function of the angular momentum J. The SM results nicely reproduce the experiment including the backbending seen at $J = 10$. On the other hand, the mean field values of E_γ follow the same trend as the experimental and SM ones but they are shifted downwards by ≈ 0.5 MeV. This means that the mean field dynamic mo-
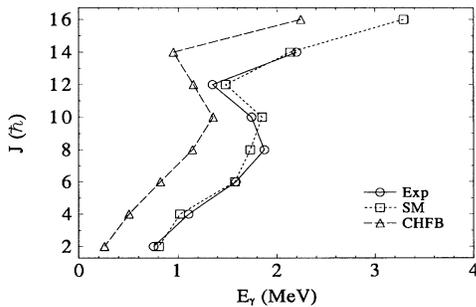
ment of inertia $[J^{(2)}(J) = 4/\Delta E_\gamma]$ is similar to the SM and experimental ones although the static moment of inertia $[J^{(1)}(J) = (2J - 1)/E_\gamma]$ is on the average a factor of 1.5 bigger. (The origin of this discrepancy will be explained later.)

Quadrupole properties.—The striking similarity between the SM and CHFB results up to the backbend can be gathered from the lower part of Fig. 2, in which the intrinsic quadrupole moment is plotted along the yrast band. The SM values are extracted from the $B(E2)$ values, assuming $K = 0$. The existence of an intrinsic state common to the members of the band can be guessed directly by calculating the contribution of a given configuration to each SM wave function (i.e., by summing the square of the amplitudes of all basic states having the same number of particles in each subshell). *These contributions are practically identical in all the eigenstates up to $J = 10$.* At higher spins rapid changes occur, and the configuration in which all the particles are in the $f_{7/2}$ orbit becomes increasingly dominant. It is clear that the intrinsic state is becoming J dependent at the backbending region, and the discrepancies in Fig. 2 beyond $J = 10$ suggest that it is no longer possible to extract an intrinsic Q_0 from the SM results, assuming a $K = 0$ band. In the upper part of the figure an alternative is proposed, by comparing the $B(E2)$ values, obtained directly in the SM case with those derived from CHFB by applying the generalization of the rotational model prescription to small triaxialities (see [5]). The agreement is again nearly perfect up to $J = 10$ but then deteriorates, although not as much as in the lower figure.

In assessing the significance of these results we should keep in mind that they are in both cases (rotational) model dependent. They indicate that the model is as good as exact up to the backbend, and then breaks down—at least in the standard implementation proposed here. They certainly *do not* indicate that the SM and CHFB
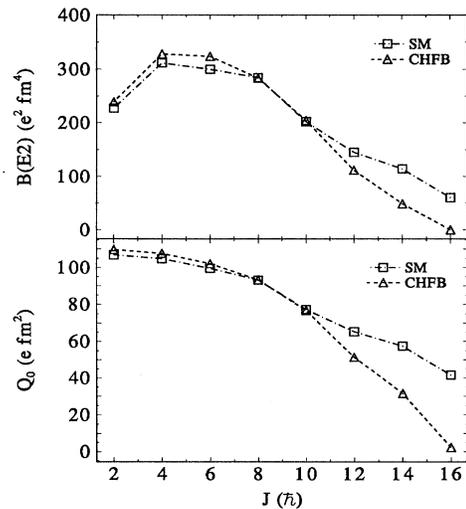

FIG. 1.   Yrast energies $E_\gamma = E(J) - E(J - 2)$.

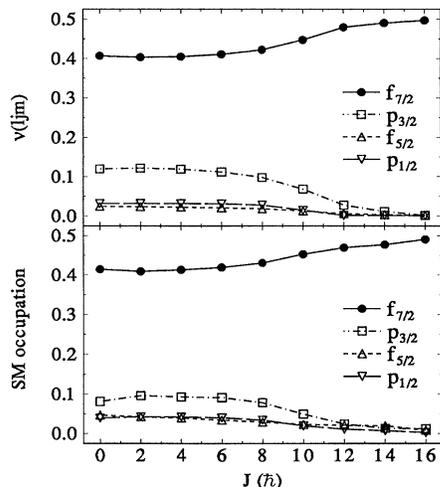FIG. 2.   Comparing $B(E2)$ and Q_0 trends.

FIG. 3. Orbital occupancies.

descriptions are becoming different. On the contrary, we shall find evidence of their closeness.

Orbital occupancies.—In Fig. 3 are plotted the fractional occupancies of the spherical orbits in the CHFB solution [Eq. (2)] (upper part) and in the SM one (lower part). In all cases they are quite constant up to the backbending where the $f_{7/2}$ orbit becomes rapidly the only relevant one.

However, the $f_{7/2}$ occupancy is *always* the largest by far, and in the CHFB case the contribution $j_x(f_{7/2})$ to $\langle J_x \rangle$ in Eq. (3) is always greater than 99%. It means that the $f_{7/2}$ orbit plays a major part in the two yrast regimes: below backbend as the major contributor to the deformed wave functions, and above through the $f_{7/2}^8$ configuration that becomes increasingly dominant. This picture is consistent with the usual idea that the backbend is associated with the alignment of $f_{7/2}$ particles, which are also massively present in the collective regime at low spin.

Magnetic properties.—In Fig. 4 we present the CHFB and SM results for the gyromagnetic factor g. In both cases and up to the backbending zone they are close to the rotational limit $g_R = Z/A = 0.50$. For a pure $f_{7/2}$ configuration the value of g is also constant and equal to
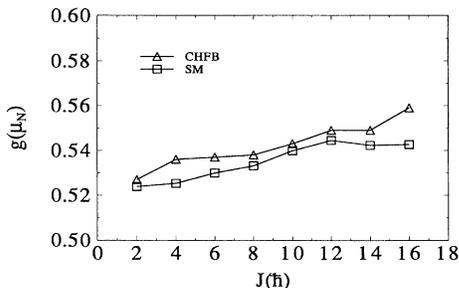
0.55, explaining the slight increase in g as we enter the backbending region where these configurations become dominant.

Pairing properties.—From all we have said, it follows that the SM and CHFB results are basically the same, except for a difference in the static moment of inertia. Its origin can be understood by redoing the SM calculations reducing the $JT = 01$ two-body matrix elements involving orbits r and t according to

$$W_{rrtt}^{01} \longrightarrow W_{rrtt}^{01} + 0.165\sqrt{(j_r + 1/2)(j_t + 1/2)}, \quad (5)$$

which amounts to subtracting a standard pairing term (j_r is the angular momentum of orbit r). The resulting E_γ pattern for an exact calculation with the modified interaction is shown as SM(E) in Fig. 5. To gain further insight we have also calculated in SM(P) the energies by taking expectation values of the modified interaction (5) using the SM wave functions obtained with KB3. [The coefficient 0.165 was chosen—somewhat arbitrarily—to make the first point coincide for CHFB and SM(P).] The conclusion is as follows: *Although the energetics of the yrast band are strongly affected by the pairing modifications, the other properties are not, since the wave functions change little.* (The overlaps $\langle SM(E), J | SM, J \rangle$ exceed 0.97 in all cases.)

As the pairing properties of the Gogny force were adjusted in a strong correlation regime (odd-even mass differences in the tin isotopes) the large static moments of inertia obtained in the CHFB calculations should be attributed to an inadequate treatment of pairing effects in a weak correlation regime rather than to the force itself: Exploratory tests using the Lipkin-Nogami approach on top of the CHFB scheme show a substantial reduction of the moment of inertia, making it much closer to the experimental data. The other intrinsic properties remain almost unaffected.

^{48}Cr *as axial rotor.*—It has been recently argued [11] that the building blocks of wave functions describing good rotors are constructed by allowing particles to move in spaces defined by $\Delta j = 2$ sequences of major shell orbits, starting on the one with the largest j. For these blocks, an approximate form of SU(3) symmetry is valid [quasi-SU(3)]. One of the predictions of this model is that ^{48}Cr
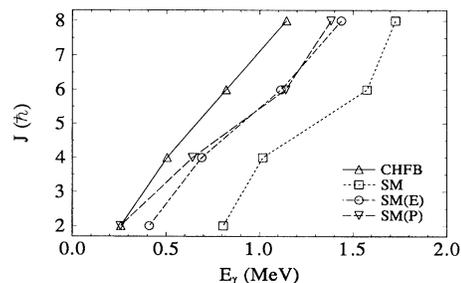

FIG. 4. Gyromagnetic ratios.

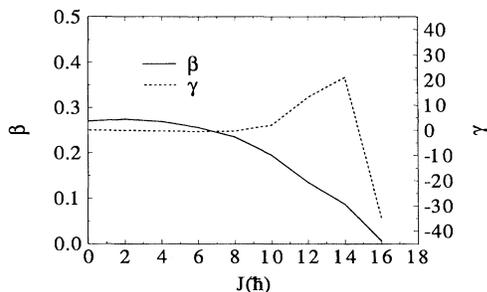FIG. 5. Influence of the pairing strength on the moment of inertia. See text.

FIG. 6.   The CHFB deformation parameters.

is an axially symmetric rotor, contrary to what happens to its counterpart in the sd shell, ^{24}Mg, that obeys Elliott's SU(3) and is triaxial. Experimentally no second 2^+ state is found in ^{48}Cr at low excitation energy, while in ^{24}Mg the second 2^+ is degenerate with the yrast 4^+. In Fig. 6 we present the values of the deformation parameters β and γ coming from the CHFB calculation.

At first, β stays constant at $\beta \approx 0.3$, while $\gamma \approx 0$, which means that ^{48}Cr behaves indeed as an axial rotor up to the backbend. Above it, as β decreases fast and the system moves to a spherical regime making it difficult to interpret in a simple way the γ behavior.

Effective charges.—Finally, we can separate from the total quadrupole moment Q_{20} in CHFB, the valence contribution Q_{20pf}(HO) by summing $q_{20}(n, l, j; n', l', j')$ in Eq. (4) over the $0f$ and $1p$ orbits, i.e., by identifying the valence orbits with harmonic oscillator ones. The ratio

$$Q_{20}/Q_{20pf}(\text{HO}) = 1.99(J = 0), \ldots, 1.83(J = 14)$$

is quite consistent with the isoscalar effective charge used in the SM calculations $q_\nu + q_\pi = 2$.

Alternatively, we can define Q_{20pf}(HF) by summing over all the values of l, j and l', j' corresponding to the pf shell, which amounts to using spherical HF orbits. This choice naturally reduces the effective charges, but they remain quite constant since

$$Q_{20}/Q_{20pf}(\text{HF}) = 1.70(J = 0), \ldots, 1.63(J = 14).$$

In conclusion, the quantitative equivalence of the SM and CHFB descriptions has two direct and welcome consequences: (i) It suggests that the Gogny force must be reasonably close to the realistic ones, consistent with *NN* data and known to yield high quality spectroscopy once their bad monopole properties are corrected. (ii) It confirms the validity of the SM choice of a model space restricted to orbits in the vicinity of the Fermi level. Clearly there is much to be gained by combining the simplicity and rigor of CHFB with the SM precision and generality.

[1] J. P. Elliott, Proc. R. Soc. London **245**, 128 (1956); **245**, 256 (1956).

[2] K. H. Bhatt and J. B. McGrory, Phys. Rev. C **3**, 1137 (1971).

[3] J. A. Cameron *et al.*, Phys. Rev. C **49**, 1347 (1994); J. A. Cameron *et al.*, Phys. Lett. B **319**, 58 (1993); T. W. Burrows, Nucl. Data Sheets **68**, 1 (1993).

[4] E. Caurier, A. P. Zuker, A. Poves, and G. Martínez-Pinedo, Phys. Rev. C **50**, 225 (1994).

[5] J. L. Egido and L. M. Robledo, Phys. Rev. Lett. **70**, 2876 (1993); J. L. Egido, L. M. Robledo, and R. R. Chasman, Phys. Lett. B **322**, 22 (1994); M. Girod, J. P. Delaroche, J. F. Berger, and J. Libert, Phys. Lett. B **325**, 1 (1994).

[6] D. Gogny, *Nuclear Selfconsistent Fields,* edited by G. Ripka and M. Porneuf (North-Holland, Amsterdam, 1975).

[7] T. T. S. Kuo and G. E. Brown, Nucl. Phys. **A114**, 241 (1968).

[8] E. Caurier, computer code ANTOINE, Strasbourg, 1989.

[9] J. F. Berger, M. Girod, and D. Gogny, Nucl. Phys. **A428**, 23c (1984).

[10] R. R. Chasman and S. Wahlborn, Nucl. Phys. **A90**, 401 (1967).

[11] A. Zuker, J. Retamosa, A. Poves, and E. Caurier, Phys. Rev. C (to be published).